

Utilization of Photoinduced Charge-Separated State of Donor–Acceptor-Linked Molecules for Regulation of Cell Membrane Potential and Ion Transport

Tomohiro Numata,^{†,‡} Tatsuya Murakami,^{‡,‡} Fumiaki Kawashima,[§] Nobuhiro Morone,[‡] John E. Heuser,[‡] Yuta Takano,[‡] Kei Ohkubo,^{||} Shunichi Fukuzumi,^{||,⊥} Yasuo Mori,^{*,†} and Hiroshi Imahori^{*,‡,§}

[†]Department of Synthetic Chemistry and Biological Chemistry, Graduate School of Engineering, Kyoto University, Nishikyo-ku, Kyoto 615-8510, Japan

[‡]Institute for Integrated Cell-Material Sciences (WPI-iCeMS), Kyoto University, Sakyo-ku, Kyoto 606-8501, Japan

[§]Department of Molecular Engineering, Graduate School of Engineering, Kyoto University, Nishikyo-ku, Kyoto 615-8510, Japan

^{||}Department of Material and Life Science, Graduate School of Engineering, Osaka University, and ALCA, Japan Science and Technology Agency (JST), Suita, Osaka 565-0871, Japan

[⊥]Department of Bioinspired Science, Ewha Womans University, Seoul 120-750, Korea

S Supporting Information

ABSTRACT: The control of ion transport across cell membranes by light is an attractive strategy that allows targeted, fast control of precisely defined events in the biological membrane. Here we report a novel general strategy for the control of membrane potential and ion transport by using charge-separation molecules and light. Delivery of charge-separation molecules to the plasma membrane of PC12 cells by a membranous nanocarrier and subsequent light irradiation led to depolarization of the membrane potential as well as inhibition of the potassium ion flow across the membrane. Photoregulation of the cell membrane potential and ion transport by using charge-separation molecules is highly promising for control of cell functions.

The integration of chemistry and biology has paved the way for new interdisciplinary science and technology that enable the control and manipulation of functions of biological systems. This methodology has been extended to explore the fusion between tailored materials and biological systems as well as protein machines and artificial systems.^{1,2} Representative examples involve the control of ion channels by photochemical switching³ and the use of biomolecular motors and pumps interfaced with synthetic systems.^{4,5}

One of the challenges in controlling biological systems at the molecular level is transporting functional molecules across barriers such as biological membranes, as such control could result in fascinating applications including sensing, detection, and drug delivery.^{1,2} In particular, the control of ion transport across cell membranes by light is fascinating because of its targeted, fast control of precisely defined events in the biological membrane. For instance, the optical control of neuronal activity^{6,7} encompasses various strategies, including photorelease of caged neurotransmitters,⁸ engineering of light-gated receptors and channels,⁹ and naturally light-sensitive ion channels.¹⁰ In these strategies, cells must be genetically

engineered to allow them to respond directly to light or to accommodate chemical modification with light-sensitive molecules. Thus, examples of the photoregulation of ion transport across biological membranes are still limited.

We focused on the nanoscale electric field of a photoinduced charge-separated (CS) state of a donor–acceptor (D–A)-linked molecule. If this linked molecule could be arranged on or in the intact biological membrane and then the CS state could be generated by photoinduced electron transfer (ET), the extremely large electric field ($\sim 10^6$ V cm⁻¹)¹¹ of the photoinduced CS state would affect electrophysiological activities in cell membranes, such as gating of voltage-gated ion channels and switching of ion transport across the membrane. Here we report the first example of photoinhibition of ion transport and subsequent depolarization in intact cells by using charge-separation molecules.

In this study, we chose ferrocene (Fc)–porphyrin (P)–C₆₀ linked triads as charge-separation molecules (Figure 1) because photoexcitation results in photoinduced ET from the porphyrin excited singlet state (¹P*) to the C₆₀ followed by a second ET from the ferrocene to the porphyrin radical cation (P^{•+}), yielding Fc⁺–P–C₆₀^{•-}, which has a long lifetime (τ) of ~ 0.01 ms and a high charge-separation efficiency of 0.25–0.99.^{12,13} To increase the affinity of the hydrophobic Fc–P–C₆₀ molecule for the phospholipid bilayer membrane, a hydrophilic cationic moiety (i.e., a tetramethylammonium group) was tethered to the ferrocene moiety of the Fc–P–C₆₀ molecule.¹⁰

The triads Fc–H₂P–C₆₀ and Fc–ZnP–C₆₀ were synthesized according to reported procedures [Figures S1 and S2 in the Supporting Information (SI)]. Porphyrin reference compounds with the cationic moiety but without the Fc and C₆₀ moieties (H₂P-ref, ZnP-ref) were also prepared (Figures S3 and S4). Synthetic procedures and characterization and optical properties are provided in the SI. Both the triads and porphyrin reference compounds were prone to precipitate from aqueous

Received: January 22, 2012

Published: March 26, 2012

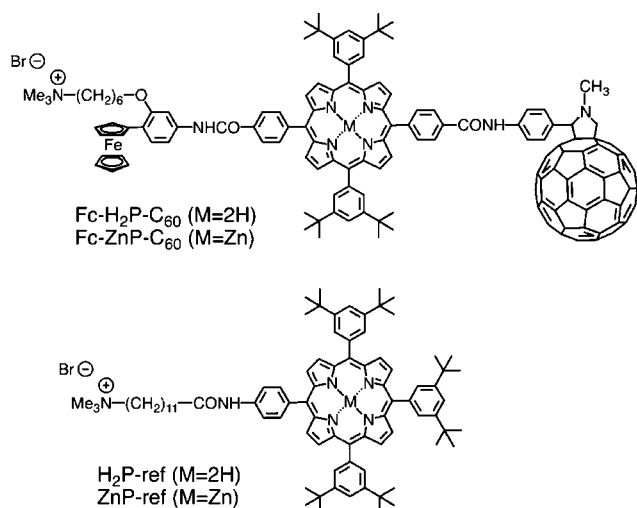


Figure 1. Molecular structures of charge-separation molecules and reference compounds used in this study.

solution, which prevented the delivery of detectable amounts of them to the cell membrane. Thus, cell-penetrating high-density lipoprotein¹⁴ (cpHDL) or a membrane fusogenic liposome¹⁵ was used as a nanocarrier for delivery to the cell membrane. HDL is believed to adopt a discoidal phospholipid bilayer circumscribed by apoA-I proteins and can incorporate hydrophobic molecules in the phospholipid bilayer. CpHDL, which was recently developed by our group as an intracellular drug delivery carrier, was prepared by mixing palmitoylcholine (POPC) and a human apoA-I mutant fused to a TAT sequence (YGRKKRRQRRR) in a 300:1 molar ratio.¹⁴ The membrane fusogenic liposome was prepared from 1-octadecanoyl-2-((9Z)-octadecenoyl)-sn-glycero-3-phosphocholine (SOPC) and 1,2-di-((9Z)-octadecenoyl)-sn-glycero-3-phosphoethanolamine (DOPE) in a 3:1 ratio.¹⁵

First, $\text{Fc-H}_2\text{P-C}_{60}$, Fc-ZnP-C_{60} , $\text{H}_2\text{P-ref}$, or ZnP-ref was incorporated into cpHDL by simply mixing them for 1 h at 37 °C. The UV-vis absorption spectra revealed a characteristic absorption arising from the porphyrin moiety, demonstrating the incorporation of the dyes into cpHDL (Figures S5 and S6). It is noteworthy that the Soret bands of the $\text{Fc-H}_2\text{P-C}_{60}$ and Fc-ZnP-C_{60} -loaded cpHDL in saline were red-shifted by ca. 10 nm relative to those of the triads in dimethyl sulfoxide (DMSO), whereas the Soret bands of $\text{H}_2\text{P-ref}$ - and ZnP-ref -loaded cpHDL revealed slight red and blue shifts, respectively, relative to those of the porphyrin references in DMSO (Figure S5). During the incorporation into cpHDL, the degree of decrease in the fluorescence of the triads was much larger for ZnP-ref than $\text{H}_2\text{P-ref}$, indicating intense aggregation of ZnP-ref compared with $\text{H}_2\text{P-ref}$ in cpHDL (Figure S6). Taking into account the solubility of the triads and the references in DMSO, these results show that the degree of aggregation increases in the order $\text{H}_2\text{P-ref} < \text{ZnP-ref} < \text{Fc-H}_2\text{P-C}_{60} < \text{Fc-ZnP-C}_{60}$.

Next, PC12 cells were treated with the dye-loaded cpHDL for 5 min at 37 °C. Confocal microscopy analysis of the PC12 cells treated with the $\text{H}_2\text{P-ref}$ -loaded cpHDL revealed that the fluorescence from the porphyrin moiety was colocalized with that from wheat germ agglutinin (WGA)-Alexa Fluor 488 conjugate that recognizes cell-surface glycans, showing the localization of $\text{H}_2\text{P-ref}$ in the vicinity of the cell membrane (Figure 2a and Figure S7c). A similar fluorescence image was

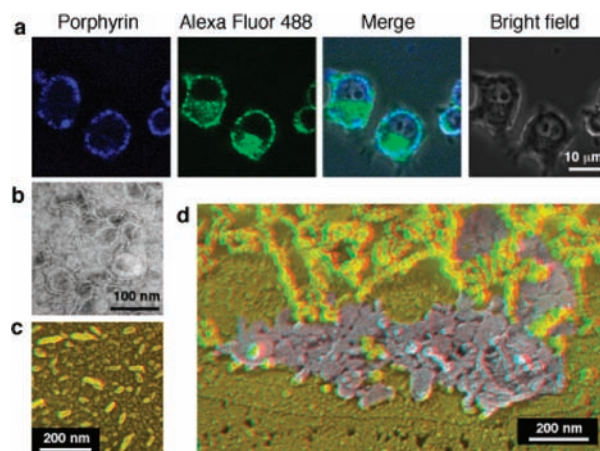


Figure 2. Cell membrane localization of $\text{Fc-H}_2\text{P-C}_{60}$. (a) Confocal microscopy images of PC12 cells treated with $\text{H}_2\text{P-ref}$ -loaded cpHDL and WGA-Alexa Fluor 488 conjugate. (b) Negatively stained electron microscopy image of $\text{Fc-H}_2\text{P-C}_{60}$ -loaded cpHDL. (c) Mica-flake electron microscopy image of $\text{Fc-H}_2\text{P-C}_{60}$ -loaded cpHDL. (d) Freeze-fracture electron microscopy image of the outer surface of the PC12 cell membrane after the treatment with $\text{Fc-H}_2\text{P-C}_{60}$ -loaded cpHDL. Clusters of discs similar to those shown in (b) are highlighted in gray.

obtained for the PC12 cells treated with the ZnP-ref -loaded cpHDL, but it was weaker because of the self-quenching of ZnP-ref arising from the aggregation described above¹⁶ (Figure S8c). In contrast, no fluorescence was observed for the PC12 cells treated with the $\text{Fc-H}_2\text{P-C}_{60}$ or Fc-ZnP-C_{60} -loaded cpHDL as a result of the intense quenching by the C_{60} via ET^{12,13} as well as the aggregation quenching (Figures S7b and S8b).¹⁶ The amount of the dye incorporated into PC12 cells, which was spectrophotometrically determined after extraction of the dye from the cells, was virtually the same for all the systems [(2–3) × 10⁷ molecules/cell]. These data indicate that the triad molecules were similarly delivered to the cell membrane.

To examine the structure of the triad-loaded cpHDL in the cell membrane, transmission electron microscopy (TEM) studies of the PC12 cells treated with the triad-loaded cpHDL were performed. As shown in Figure 2b,c, $\text{Fc-H}_2\text{P-C}_{60}$ -loaded cpHDL was found to have a discoidal shape with a thickness of ~5 nm, analogous to that of empty HDLs, and some of the discs were stacked to create lamellar structures. The disks ranged from 60 to 80 nm in diameter, which was much larger than that of physiologically relevant discoidal HDLs (~10 nm). Our previous report showed that discoidal HDL can be enlarged more than 10-fold by loading with hydrophobic molecules when prepared with an increased amount of POPC (250:1 molar ratio of POPC to apoA-I).¹⁷ As the cpHDL used in this study was prepared at a 300:1 molar ratio, this enlargement could be explained by $\text{Fc-H}_2\text{P-C}_{60}$ loading.

Next, freeze-fracture electron microscopy was applied to visualize $\text{Fc-H}_2\text{P-C}_{60}$ -loaded cpHDL in the cell membrane. This technique does not need chemical fixation of cells, which affects the cellular location of TAT peptide conjugates. Figure 2d shows a fractured surface in the vicinity of the outer cell membrane of the PC12 cells treated with $\text{Fc-H}_2\text{P-C}_{60}$ -loaded cpHDL. The 60–80 nm discs were observed as planar clusters located on the outer cell membrane. This clustering is consistent with the observation of the dotted fluorescence of

H₂P-ref in Figure 2a as well as the intense aggregation behavior of Fc-H₂P-C₆₀. Thus, it could be concluded that Fc-H₂P-C₆₀ was delivered to the surface of the outer cell membrane by cpHDL. On the other hand, we did not obtain images indicating incorporation of Fc-H₂P-C₆₀ inside the cell membrane.

Photoinduced changes in the membrane potential at 25 °C were examined using patch clamp technique. After 3 min of treatment of PC12 cells with the dye-loaded cpHDL, visible-light illumination (400–450 nm) was started under the current clamp. When the PC12 cells were treated with the Fc-H₂P-C₆₀-loaded cpHDL, depolarization of the membrane potential occurred gradually with time, reaching a constant membrane potential (depolarization = 13 mV) in 1 min (Figure 3a). The

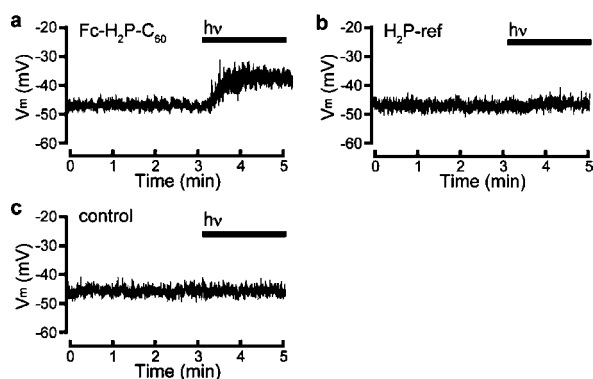


Figure 3. Photoinduced depolarization of PC12 cells containing Fc-H₂P-C₆₀. Representative traces of time-dependent changes in the membrane potential under illumination (400–450 nm, input power 5 mW cm⁻²) are shown for PC12 cells treated for 3 min with (a) Fc-H₂P-C₆₀-loaded cpHDL, (b) H₂P-ref-loaded cpHDL, or (c) medium only and then washed with phosphate-buffered saline.

degree of depolarization did not alter in PC12 cells treated with a larger amount of Fc-H₂P-C₆₀-loaded cpHDL. On the other hand, under the illumination neither PC12 cells themselves nor the cells treated with cpHDL loaded with H₂P-ref, which was unable to undergo charge separation, showed change in the membrane potential (Figure 3b,c). Therefore, the photoinduced changes in membrane potential observed here clearly occurred through the CS state of Fc-H₂P-C₆₀ under illumination (Figures S9 and S10).¹⁸

Like cpHDL, the well-established SOPC-DOPE fusogenic liposome,¹⁵ the diameter of which was determined to be 60 nm with a second population of 200 nm (Figure S11), delivered Fc-H₂P-C₆₀ to the PC12 cell membrane (Figure S7d). In fact, it led the analogous photoinduced depolarization (Figure S12a). These results support the delivery of Fc-H₂P-C₆₀ to the cell membrane by cpHDL.

Next, photoinduced changes in membrane current were evaluated using the voltage clamp method. Under illumination (Figure 4a, bar) the membrane current of PC12 cells treated with the Fc-H₂P-C₆₀-loaded cpHDL decreased gradually to reach a plateau (Figure 4a). The current-voltage profile (Figure 4b, x) and the reversal potential of -70 mV¹⁹ (Figure 4b inset, x) are typical characteristics of voltage-gated potassium channels.²⁰ Under the illumination, the reversal potential was significantly increased (Figure 4b inset, y), suggesting inhibition of potassium ion transport. In addition, this effect of illuminated Fc-H₂P-C₆₀ was ablated by cotreatment with a potassium channel inhibitor, tetraethylam-

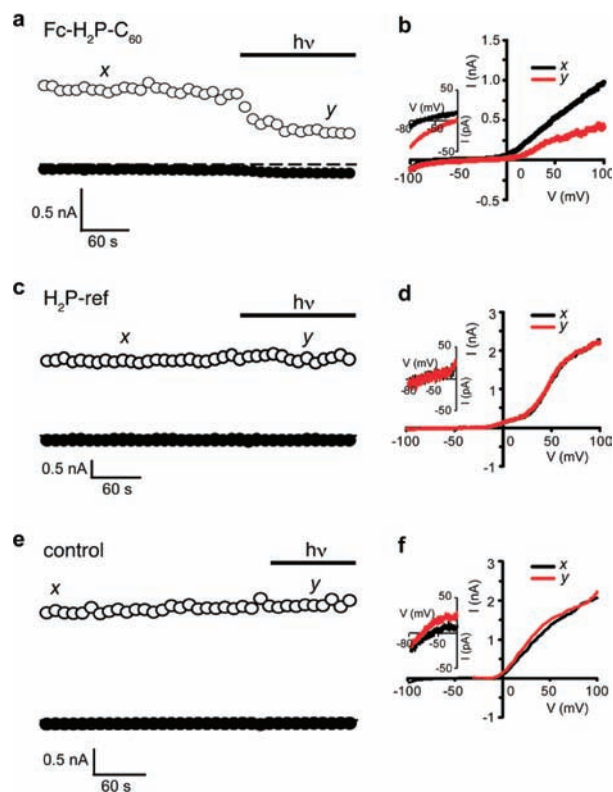


Figure 4. Photoinduced change in membrane current of PC12 cells containing Fc-H₂P-C₆₀. Representative traces of time-dependent changes in the membrane current (a, c, e) and *I*-*V* curve (b, d, f) under illumination (400–450 nm, input power 5 mW cm⁻²) are shown for PC12 cells treated with Fc-H₂P-C₆₀-loaded cpHDL. The black and red curves in (b), (d), and (f) were collected at the time points indicated by x and y, respectively, in (a), (c), and (e). The insets in (b), (d), and (f) show magnified views around the *V*-axis intercept.

monium bromide (TEA) (Figure S13). Given no rectification under the conditions of y in Figure 4b, the depolarization observed in Figure 3a may result from the deactivation of the voltage-gated potassium channels.

Some types of porphyrins have been clinically used for photodynamic therapy, in which singlet oxygen (¹O₂) is generated via energy transfer from the porphyrin excited triplet state to O₂ and attacks cancer cells.²¹ In the process of cell killing, ¹O₂ produces oxidative cell membrane damage followed by the depolarization of the membrane potential.²² Thus, the possible involvement of ¹O₂ in the photoinduced depolarization observed here was assessed using Singlet Oxygen Sensor Green Reagent (SOSG) (Invitrogen)²³ for Fc-H₂P-C₆₀ and H₂P-ref in DMSO (Figure S14). After the light illumination at 400–450 nm, Fc-H₂P-C₆₀ did not enhance the SOSG fluorescence, whereas H₂P-ref enhanced the SOSG fluorescence significantly, implying that the ¹O₂ generation efficiency of H₂P-ref is much higher than that of Fc-H₂P-C₆₀. In agreement with these data, phototoxicity of Fc-H₂P-C₆₀ delivered to the PC12 cell membrane was not detected after 4.5 min illumination, whereas all the cells loaded with H₂P-ref were propidium iodide (PI)-positive (Figure S15), which suggests that the cell membrane was damaged heavily enough to allow PI influx across it. This high phototoxicity of H₂P-ref would be due to its photodynamic effect. Taking into account the fact that the depolarization was observed only in the treatment with the

Fc-H₂P-C₆₀-loaded cpHDL, we could conclude that ¹O₂-induced membrane damage is not involved in the depolarization observed in this study.

Similar depolarization behavior was noted for the PC12 cells treated with the Fc-ZnP-C₆₀-loaded cpHDL (Figure S16), but the degree of the depolarization (9 mV) was smaller than for Fc-H₂P-C₆₀-loaded cpHDL. This result appears to contradict the consideration that the depolarization occurred through the CS state of Fc-H₂P-C₆₀ under illumination, as the charge-separation efficiency of Fc-ZnP-C₆₀ (0.99) is higher than that of Fc-H₂P-C₆₀ (0.25) in benzonitrile solution.^{12,13} One explanation for this discrepancy is that the charge-separation efficiency is largely attenuated by aggregation of the charge-separation molecules. As described above, Fc-ZnP-C₆₀ has an increased tendency to aggregate in cpHDL and DMSO in comparison with Fc-H₂P-C₆₀. Thus, the intense aggregation of Fc-ZnP-C₆₀ on the membrane surface may quench ¹ZnP* or deactivate the CS state, decreasing the effect of the CS state on the membrane potential.

PC12 cells show a sharp increase in the membrane potential in response to physiological stimuli.²⁴ Relative to such stimuli, illuminated Fc-H₂P-C₆₀ slowly altered the membrane potential (Figure 3a), although the CS state of Fc-H₂P-C₆₀ is formed in ~1 ns after the illumination.^{12,13} In addition, the depolarization induced by the illuminated Fc-H₂P-C₆₀ was not reversible. At present, the reasons for these behaviors are not clear, but slow dynamic movement of the charge-separation molecules on the membrane surface may be induced by the initial resting potential of -70 mV, eventually yielding a direct interaction between the voltage-gated potassium channels and the charge-separation molecules.

In conclusion, we have successfully controlled the membrane potential and ion transport across the PC12 cell membrane by using ferrocene-porphyrin-fullerene triad molecules, cell-penetrating HDL, and light. The results obtained here provide valuable and fundamental information on interactions between the photoinduced CS state and the biological membrane. More importantly, this is the first optogenetic method utilizing the photoinduced CS state of D-A-linked molecules on the intact cell membrane. It should also be noted that our membranous nanocarrier, cpHDL, enabled the efficient delivery of the triad to the outer surface of the intact cell membrane. Photo-regulation of the cell membrane potential and ion transport across the membrane using charge separation is a potential strategy for controlling cell functions in a spatiotemporal manner that might be useful for activating neuronal cells. At present, the degree of polarization and photoreversibility is insufficient to control the firing of neuronal cells, but further sophisticated molecular design of charge-separation molecules will allow us to achieve such events using light.

■ ASSOCIATED CONTENT

● Supporting Information

Experimental details and additional figures. This material is available free of charge via the Internet at <http://pubs.acs.org>.

■ AUTHOR INFORMATION

Corresponding Author

mori@sbchem.kyoto-u.ac.jp; imahori@scl.kyoto-u.ac.jp

Author Contributions

[#]These authors contributed equally.

Notes

The authors declare no competing financial interest.

■ ACKNOWLEDGMENTS

This work was supported by the WPI Initiative of MEXT, Japan, and in part by a Health Labor Sciences Research Grant (nano-001 to N.M.) and by Innovative Areas, MEXT (N.M.), and NRF/MEST of Korea through WCU(R31-2008-000-10010-0) and GRL (2010-00353) Programs (S.F.).

■ REFERENCES

- (1) Shoseyov, O.; Levy, I. *Nanobiotechnology: Bioinspired Devices and Materials of the Future*; Humana Press: Totowa, NJ, 2010.
- (2) Miller, A. D.; Tanner, J. *Essentials of Chemical Biology: Structure and Dynamics of Biological Macromolecules*; Wiley: Chichester, U.K., 2008.
- (3) Koçer, A.; Walko, M.; Meijberg, W.; Feringa, B. L. *Science* **2005**, *309*, 755.
- (4) van den Heuvel, M. G. L.; Dekker, C. *Science* **2007**, *317*, 333.
- (5) Steinberg-Yfrach, G.; Rigaud, J.-L.; Durantini, E. N.; Moore, A. L.; Gust, D.; Moore, T. A. *Nature* **1998**, *392*, 479.
- (6) Szobota, S.; Isacoff, E. Y. *Annu. Rev. Biophys.* **2010**, *39*, 329.
- (7) Fiala, A.; Suska, A.; Schlüter, O. M. *Curr. Biol.* **2010**, *20*, R897.
- (8) Lima, S. Q.; Miesenböck, G. *Cell* **2005**, *121*, 141.
- (9) Banghart, M.; Borges, K.; Isacoff, E.; Trauner, D.; Kramer, R. H. *Nat. Neurosci.* **2004**, *7*, 1381.
- (10) Nagel, G.; Ollig, D.; Fuhrmann, M.; Kateriya, S.; Musti, A. M.; Bamberg, E.; Hegemann, P. *Science* **2002**, *296*, 2395.
- (11) Gosztola, D.; Yamada, H.; Wasielewski, M. R. *J. Am. Chem. Soc.* **1995**, *117*, 2041.
- (12) Imahori, H.; Tamaki, K.; Guldi, D. M.; Luo, C.; Fujitsuka, M.; Ito, O.; Sakata, Y.; Fukuzumi, S. *J. Am. Chem. Soc.* **2001**, *123*, 2607.
- (13) Imahori, H.; Yamada, H.; Nishimura, Y.; Yamazaki, I.; Sakata, Y. *J. Phys. Chem. B* **2000**, *104*, 2099.
- (14) Murakami, T.; Wijagkanalan, W.; Hashida, M.; Tsuchida, K. *Nanomedicine (London)* **2010**, *5*, 867.
- (15) Ba, H.; Rodríguez-Fernández, J.; Stefani, F. D.; Feldman, J. *Nano Lett.* **2010**, *10*, 3006.
- (16) Imahori, H.; Hosomizu, K.; Mori, Y.; Sato, T.; Ahn, T. K.; Kim, S. K.; Kim, D.; Nishimura, Y.; Yamazaki, I.; Ishii, H.; Hotta, H.; Matano, Y. *J. Phys. Chem. B* **2004**, *108*, 5018.
- (17) Murakami, T.; Tsuchida, K.; Hashida, M.; Imahori, H. *Mol. Biosyst.* **2010**, *6*, 789.
- (18) Formation of the CS state of Fc-H₂P-C₆₀ in DMSO ($\tau = 5.5 \mu\text{s}$) as well as in the deaerated aqueous solution containing PC12 cells treated with Fc-H₂P-C₆₀-loaded cpHDL ($\tau = 3.0 \mu\text{s}$) was confirmed by transient absorption measurements (Figures S9 and S10).
- (19) McDaniel, S. S.; Platoshyn, O.; Yu, Y.; Sweeney, M.; Miriel, V. A.; Golovina, V. A.; Krick, S.; Lapp, B. R.; Wang, J.-Y.; Yuan, J. X.-J. *J. Appl. Physiol.* **2001**, *91*, 2322.
- (20) Bae, Y. M.; Kim, A.; Kim, J.; Park, S. W.; Kim, T.-K.; Lee, Y.-R.; Kin, B.; Cho, S. I. *Biochem. Biophys. Res. Commun.* **2006**, *347*, 468.
- (21) Pass, H. I. *J. Natl. Cancer Inst.* **1993**, *85*, 443.
- (22) Stark, G. J. *Membr. Biol.* **2005**, *205*, 1.
- (23) Flors, C.; Fryer, M. J.; Waring, J.; Reeder, B.; Bechtold, U.; Mullineaux, P. M.; Nonell, S.; Wilson, M. T.; Baker, N. R. *J. Exp. Bot.* **2006**, *57*, 1725.
- (24) Conforti, L.; Millhorn, D. E. *J. Physiol.* **1997**, *502*, 293.